J Solid State Electrochem (2012) 16:235–245
DOI 10.1007/s10008-011-1319-6

ORIGINAL PAPER

Syntheses and modifications of bisdiazonium salts of 3,8-benzo[*c*]cinnoline and 3,8-benzo[*c*]cinnoline 5-oxide onto glassy carbon electrode and the characterization of the modified surfaces

Aybüke A. İsbir-Turan · Emine Kılıç · Zafer Üstündağ · Haslet Ekşi · Ali Osman Solak · Betül Zorer

Received: 17 June 2010 / Revised: 29 November 2010 / Accepted: 12 December 2010 / Published online: 8 February 2011

Abstract The goal of this study was to prepare novel glassy carbon electrode surfaces using two similar *bis*-diazonium salts, 3,8-benzo[*c*]cinnoline (3,8-BCC-BDAS) and 3,8-benzo[*c*]cinnoline 5-oxide (3,8-BCCNO-BDAS) at the glassy carbon (GC) surface. These diazonium salts were reduced electrochemically and covalently electrografted onto the glassy carbon electrode surface to form modified electrodes. Electrochemical reduction of 3,8-BCC-BDAS and 3,8-BCCNO-BDAS salts on the electrode surface yielded a compact and stable film. The existence of BCC moieties on the GC surface was characterized by X-ray photoelectron spectroscopy, reflectance-adsorption infrared spectroscopy, cyclic voltammetry, ellipsometry, and electrochemical impedance spectroscopy. The stability and working potential range of the novel modified electrodes were also studied. The possibility of analytical application of these novel surfaces for inorganic cations and especially selectivity to copper ions was investigated. 3,8-diaminobenzo[*c*]cinnoline (3,8-DABCC) and its 5-oxide derivative (3,8-DABCCNO) were synthesized from the reductive cyclization of 2,2′-dinitrobenzidine and prepared their bisdiazonium salts via the tetrazotization reactions of the diamines with $NaNO_2$. The structures of 3,8-DABCC and 3,8-DABCCNO and their corresponding bisdiazonium salts are confirmed by spectral analysis.

Keywords 3,8-Benzo[*c*]cinnoline · Reflectance-adsorption infrared spectroscopy · X-ray photoelectron spectroscopy · Ellipsometry · Electrochemical impedance spectroscopy

A. A. İsbir-Turan · E. Kılıç · H. Ekşi · A. O. Solak (✉) · B. Zorer
Faculty of Science, Department of Chemistry, Ankara University,
06100 Tandogan,
Ankara, Turkey
e-mail: aliosman.solak@gmail.com

Z. Üstündağ
Faculty of Art and Sciences, Department of Chemistry,
Dumlupınar University,
Kütahya, Turkey

A. O. Solak
Faculty of Engineering, Department of Chemical Engineering,
Kyrgyz-Turk Manas University,
Bishkek, Kyrgyzstan

Introduction

Recently, during the past years, chemically modified electrodes have gained attention because of their wide potential use in analytical and technical applications [1]. The substrates of the modified electrodes have been mostly carbon-based materials and metals such as gold, platinum, and iron [2]. A variety of chemical and electrochemical techniques have been used to graft the organic molecules to the substrate with the most versatile and widely studied technique being the organic self-assembly films formed on gold surfaces for various purposes [3]. Other techniques include amine ($-NH_2$) oxidation [4, 5], oxidation in the presence of alcohols [6], conductive polymer formation [7], Langmuir-Blodgett film formation [8], and aryl diazonium salt reduction [9]. Electrochemical reduction of aryl diazonium salts in aqueous and nonaqueous media produces highly reactive phenyl radicals that irreversibly bind to the carbon and metal surfaces [10–15]. The high reactivity of phenyl radicals produces compact organic layers on carbon and metal substrates. Some advantages of the aryl diazonium salt reduction method are its low cost and easy applicability in the preparation of modified electrodes [2]. Forming covalent bonds on carbon, metal, and/or metal

oxide surfaces using various diazonium salts is getting more popular in the area of molecular electronics and sensing applications [16]. McCreery et al. [17] fabricated molecular electronic junctions by covalent bonding onto a graphitic carbon substrate; they characterized this novel surface using Raman spectroscopy and investigated its conductance and electrical properties. Derivatized conducting surfaces with biomolecules are used in biosensing. Reversible trapping of ionic waste on electrografted surfaces is used as an alternative to ion-exchange resins [18–20].

Characterization of modified surfaces can be achieved using electrochemical methods such as cyclic voltammetry (CV) [11] and electrochemical impedance spectroscopy (EIS) [12], spectroscopic methods such as X-ray photoelectron spectroscopy (XPS) [17], electron spin resonance [21] and Raman spectroscopy [12], time-of-flight secondary ion mass spectroscopy (ToF-SIMS) [16], and microscopic methods such as atomic force microscopy [22], scanning tunneling microscopy [23], scanning electrochemical microscopy [24], ellipsometry [25], and surface plasmon resonance techniques [26].

Benzo[*c*]cinnolines are an important group of compounds which can be used as intermediates in the production of dyes [27], colored polymers [28, 29], dye bleach catalyst [30], photoconducters [31], and photosentiziers [32]; besides, BCC and some of its derivatives have mutagenic [33] and herbicidal activities [34].

Although there are a variety of methods published about the synthesis of benzo[*c*]cinnoline (BCC) and its 5-oxide (BCCNO) derivative [35–38] a few papers have been recorded dealing with the synthesis of 3,8-diaminobenzo[*c*]cinnoline that has been produced from 2,2′-dinitrobenzidine by electroreduction [39], or the reduction with $LiAlH_4$ [40] or the catalytic hydrogenation on Pd-Al_2O_3 [29]. A paper was published in 1992, including the synthesis of 3,8-bisazobenzo[*c*]cinnoline 5-oxide derivatives, from the coupling reactions of the bisdiazonium salt of 3,8-diaminobenzo-[*c*]cinnoline 5-oxide with phenolic coupling components, and about their usage as sensitizer of electrophotographic devices [32]. As far as we know there is no detailed procedure for the synthesis of 3,8-diaminobenzo[*c*]cinnoline 5-oxide (3,8-DABCCNO) in the literature.

The goal of the present work was to prepare novel surfaces with benzo[*c*]cinnoline-3,8-bis(diazonium) bis(tetrafluoroborate) (3,8-BCC-BDAS) and benzo[*c*]cinnoline-3,8- bis(diazonium) 5-oxide bis(tetrafluoroborate) (3,8-BCCNO-BDAS) to get a new look at the glassy carbon (GC) modification area. For this aim, firstly, 3,8-DABCC and its 5-oxide derivative (3,8-DABCCNO) were synthesized from the reductive cyclization of 2,2′-dinitrobenzidine with hydrazinehydrate and Pd-C (10%Pd) as catalyst and prepared their tetrazonium salts via the tetrazotization reactions of the diamines with $NaNO_2$. The structures of 3,8-DABCC and 3,8-DABCCNO and their corresponding bisdiazonium salts are comfirmed by spectral analysis.

Materials and methods

Chemicals, instrumentation and procedures

All chemicals were reagent grade and used as received and included the following: acetonitrile (MeCN) (Sigma-Aldrich), isopropyl alcohol (IPA) (Sigma-Aldrich), dopamine (DA) (Fluka), $AgNO_3$ (Fluka), activated carbon (Sigma-Aldrich), tetrabutylammoniumtetrafluoroborate (TBATFB) (Fluka), hexaammineruthenium(III) chloride (Sigma-Aldrich), potassium ferricyanide $K_3Fe(CN)6$ (Sigma-Aldrich), potassium ferrocyanide $K_4Fe(CN)_6$ (Sigma-Aldrich), potassium chloride (Merck), sulphuric acid (Carlo-Erba) and ferrocene (Fc) (Sigma). Solutions were degassed with purified argon (99.999%) for at least 10 min before use and an argon atmosphere was maintained over the solutions throughout the electrochemical experiments. A nitrogen gas stream was used to dry the cleaned and polished GC surfaces before the modification processes. All the processes performed in aqueous media for example, preparation of the aqueous solutions, glassware cleaning and polishing of the GC were carried out in ultra pure quality water with a resistance of ~18.3 MΩ cm (Human Power I^+ Scholar purification system). All experiments were performed at room temperature.

All electrochemical experiments were performed with a CV-50W electrochemical analyzer (Bioanalytical System Inc. Lafayette, IL, USA) equipped with a BAS C3 cell stand and Gamry Reference 600 workstation. BAS Model MF-2012 GC and Tokai GC-20 electrodes were modified with 3,8-BCC-BDAS and 3,8-BCCNO-BDAS to obtain 3BCC-GC and 3BCCNO-GC modified GC working electrodes, respectively. Either an $Ag/AgCl/KCl_{(sat.)}$ or an Ag^+/Ag (0.01 M in MeCN and 0.1 M TBATFB) was used as reference electrode. Pt wire was the counter electrode.

EIS experiments were carried out with a Gamry Reference 600 workstation using EIS 300 Gamry software. The GC electrodes before and after modification were characterized in a 2 mM $Fe(CN)_6^{3-/4-}$ redox couple via EIS methods. EIS data were measured between 100 kHz and 0.1 Hz at a 10 mV ac wave amplitude and at an electrode potential of 0.215 V, which is the formal potential of a $Fe(CN)_6^{3-/4-}$ redox couple. Experimental data of the electrochemical impedance plot were analyzed by applying the nonlinear least squares fitting to the theoretical model represented by an equivalent electrical circuit.

Ellipsometric measurements of the film thickness were performed with an ELX-02C/01R high precision discrete wavelength ellipsometer. The wavelength was 532 nm for

all experiments. The thickness values of 3BCC-GC and 3BCCNO-GC films at the platinum surface were determined from the average of the measurements using an incidence angle of 70°.

IRRAS spectra of the organic molecules in both solid and monolayer forms were collected at room temperature (Bruker Tensor 27 FT-IR). The spectra of the solids were obtained in KBr pellets using transmission mode and a room-temperature DTGS detector by averaging 32 scans. The IR spectra of 3BCC-GC and 3BCCNO-GC tethered to the graphitic surfaces were obtained using a Ge total reflection accessory (GATR; 65° incident angle relative to surface normal, Harrick Scientific) and a liquid N_2-cooled MCT detector averaging 256 scans. All spectra of the monolayers were obtained using p-polarized radiation [41].

Cleaning process and glassy carbon electrode preparation

BAS Model MF-2012 and Tokai GC-20 glassy carbon electrodes (a disk with 2 mm thickness) were used in the modification and characterization processes. The geometric area of the former was 0.071 cm^2 and O-ring delimited area of the latter was 0.30 cm^2. GC electrodes were prepared by polishing them to a mirror-like finish with fine wet emery paper (grain size 4000). They were polished successively in 0.3 μm and 0.05 μm alumina slurries on microcloth pads (Buehler, Lake Bluff, IL, USA). GC electrodes were sonicated in an ultrasonic bath (Bandelin Sonorex) first in ultra pure water and then in a 1:1 (v/v) isopropyl alcohol (IPA) and acetonitrile (MeCN) mixture for 10 min. IPA and MeCN were purified with an equal volume of activated carbon filtered through Whatman filter paper No. 1 before use. GC electrodes were rinsed with pure acetonitrile and subjected to a nitrogen gas stream to remove any dust residue and to dry the electrode surface before derivatization.

Synthesis of 3,8-diaminobenzo[c]cinnoline (3,8-DABCC)

After the addition of 10 M NaOH (15 mL) to a hot mixture of 2,2′-dinitrobenzidine (2.80 g, 10.2 mmol), Pd-C (0,20 g; Pd 10%) in EtOH (60 mL), hyrazine hydrate (6.5 mL, 100%) was added dropwise, and the mixture was refluxed for 2 1/2 h. The hot reaction mixture was filtered, and the solution was diluted with water. The precipitated product was filtered off, washed with water and dried in air. The crude product was crystallized from H_2O. The yield was 1.45 g (70%), mp. 268–269 °C. Reported mp. is 268 °C [29] FTIR (cm^{-1}, in KBr disk) : 3320, 3204 (N-H), 1619, 1481, 1393, 1314, 1199, 1131, 847, 811,743, 696. ^{1}H NMR (400 MHz, DMSO-d_6) : δ 8.08 (d, 1 H, *J*=8.87 Hz, H-1), 7.19 (d, 1 H, *J*=2.23 Hz, H-4), 6.96 (dd, 1 H, *J*=8.80, *J*=2.20 Hz, H-2), 5.94 (bs, 2 H, NH_2). GC-MS (70 eV) : m/z 210 (M^+; 100%), 211 (*M*+1; 15%).

Synthesis of 3,8-diaminobenzo[c]cinnoline 5-oxide (3,8-DABCCNO)

To the boiling mixture of 2,2′-dinitrobenzidine (2.80 g, 10,2 mmol), sodium carbonate (0.50 g) and Pd-C on charcoal (0,20 g; Pd 10%) in 50 mL alcohol was added hyrazine hydrate (5 mL, 100%) dropwise during 1/2 h, and refluxed for 2 h. The precipitated product was filtered off, washed with water and alcohol, and dried in air. The crude product was crystallized from DMF. The yield was 1.40 g (61%), mp. 284–285 °C (dec). FTIR (cm^{-1}, in KBr disk): 3420, 3337 and 3222 (N-H), 1627, 1545, 1485, 1403, 1327, 1224, 820, 719, 612. ^{1}H NMR (400 MHz, DMSO-d_6): δ 8.25 (d, 1 H, *J*=8.8 Hz, H-1), 8.12 (d, 1 H, *J*=8.8 Hz, H-10), 7.55 (d, 1 H, *J*=2.4 Hz, H-4), 7.26 (dd, 1 H, *J*=8.8, *J*=2.4 Hz, H-2), 7.04 (dd, 1 H, *J*=8.8, *J*=2,4 Hz, H-9), 6.84 (d, 1 H, *J*=2.4 Hz, H-7), 6.03 (bs, 2 H, 3-NH_2), 5.72 (bs, 2 H, 8-NH_2). API-ESMS (100 eV): m/z 227 (M+H; 100%), 210 (M-16; 16%).

Synthesis of benzo[c]cinnoline-3,8-bis(diazonium) bis(tetrafluoroborate) (3,8-BCC-BDAS)

3,8-DABCC (0.21 g, 1 mmol) was dissolved in AcOH (2.5 mL). Water (5 mL) and concentrated HCl (2.5 mL) were added to this solution, respectively. To the mixture cooled at about 0 °C, $NaNO_2$ solution (0.20 g, 2.9 mmol; in 1 mL H_2O) was added dropwise with stirring continously. The reaction mixture set aside for 1 h at 0 °C, and then filtered. To the resulting filtrate was added 1 mL of HBF_4 (50%), and the separated product was collected by filtering, washed with cold water, alcohol and diethylether. The yield was 0.22 g (54%). FTIR (cm^{-1}, in KBr disk): 3106, 2306 (N_2^+), 1599, 1456, 1412, 1347, 1294, 1070 (BF_4^-), 821, 768, 680.

Synthesis of benzo[c]cinnoline-3,8-bis(diazonium) 5-oxide bis(tetrafluoroborate) (3,8-BCCNO-BDAS)

The work-up procedure was the same that given for 3,8-BCC-DAS. The reaction was proceeded by use of 3,8-DABCCNO (0.23 g, 1 mmol), 8 mL H_2O, 2 mL conc. HCl, $NaNO_2$ (0.20 g, 2.9 mmol; in 1 mL H_2O) and 1 mL of HBF_4 (50%). The yield was 0.30 g (71%). FTIR (cm^{-1}, in KBr disk): 3118, 2307 (N_2^+), 1601, 1499, 1459, 1411, 1333, 1260, 894, 820.

Results and discussions

Synthesis of the bisdiazonium modifiers and their amino precursors

3,8-DABCC and 3,8-DABCCNO were prepared from the reduction of 2,2′-dinitrobenzidine with hydrazine hydrate in

ethanol using Pd-C(10% Pd) as catalyst, with the yields 70% and 61%, respectively. When the reaction was promoted in aq. alcoholic NaOH solution 3,8-DABCC was obtained, but in less basic media including Na_2CO_3, 3,8-DABCCNO was the main product. The structures of the products were confirmed by analyzing their HNMR, mass and FTIR spectra. The H,H COSY experiment of 3,8-DABCCNO was also used for assignments. The characteristic FTIR peaks of 3,8-DABCC and 3,8-DABCCNO are at 3320 and 3204, and 3420, 3337 and 3222 cm^{-1} are attributed to N-H stretching vibrations of amino groups, respectively. The stretching vibrations of N-H at 3420 cm^{-1} is probably due to non H-bonded N-H as 3,8-DABCCNO is less basic character than 3,8-DABCC. The bands at about 1620 and 1480 cm^{-1} are assigned to C=C (stretc.), and N-H (bend.), and N=N (stretc.) vibrations, respectively. In the FTIR spectra of 3,8-BCC-BDAS and 3,8-DABCCNO-BDAS, two peaks emerged at 2306 and 2307 cm^{-1}, respectively, are attributed to stretching of diazonium groups, and the peaks of amino grups in DABCC and DABCCNO at about 3400-3200 cm^{-1} are dissappeared.

In the ^{1}H NMR spectrum of DABCC; the doublets at 8.08 and 7.19 ppm are assigned to H-1 and H-4, respectively. The absorbtion of H-2 is observed as doublets of doublet at 6.96 ppm. A broad peak at 5.94 ppm for two hydrogens belongs to NH_2. As expected the unsymmetrical structure of 3,8-DABCCNO, eight absorbtion peaks are observed in its ^{1}H NMR spectrum. The peaks are assigned by means of H,H-COSY experiment. The peaks at 8.25, 7.55 and 7.26 ppm belong to H-1, H-4 and H-2; the peaks at 8.12, 7.04 and 6.84 ppm are attributed to H-10, H-9 and H-7, respectively. Two broad bands appeared at 6.03 and 5.72 ppm are attributed to amino groups at positions 3 and 8, respectively. The hydrogens, H-4 and 3-NH_2, are more deshielded than H-7 and 8-NH_2, respectively, because of deshielding effect of positively charged atom N-5.

Electrografting 3,8-BCC-BDAS and 3,8-BCCNO-BDAS onto glassy carbon electrodes

GC electrodes were modified with 3,8-BCC and 3,8-BCCNO bisdiazonium salts via electrochemical reduction in MeCN containing 0.1 M TBATFB. These molecules were grafted onto the GC surface using a cyclic voltammetric technique forming covalent bonds between the molecules and the substrate [16]. By scanning between +0.5 and −0.8 V, the bisdiazonium salts were reduced electrochemically and reacted with the polished glassy carbon surface to form a compact film, as shown in Scheme 1 for only 3,8-BCC-BDAS. One of the diazo functionalities of the diazonium salt was probably reduced at the one end, forming a reactive radical to attact the carbon surface. The diazo group at the other end probably underwent a hydro-dediazoniation process by residual water either in the solution or after the attachment of the radical to the GC surface [42]. Since the radical is very reactive, the kinetics of the attachment process is higher than the hydro-dediazoniation process of the unreduced diazo groups. Therefore, we assume that the hydro-dediazoniation of the remaining diazo group occurred at the surface, replacing the diazo group by a proton from a proton donor, probably residual water in MeCN. Raman spectra show no diazo group band on the GC surface after the modification process, as will be discussed later.

Figure 1 shows the modification voltammogram for the attachments of 1 mM 3,8-benzo[*c*]cinnoline and 1 mM 3,8-benzo[*c*]cinnoline N-oxide at the GC surface in MeCN containing 0.1 M TBATFB. Although the general appearances of Fig. 1a and b are similar, their Ep and Ip values and the voltammetric wave shapes differ from each other, arising probably from the diffusional, adsorptional and kinetic differences of 3,8-BCC-BDAS and 3,8-BCCNO-BDAS during the reduction process. The voltammograms are very characteristic of the reduction of diazonium species with an irreversible cathodic peak in the first scan. The surfaces were passivated during the first scan, forming a compact film for both molecules. In the second scan, the reduction wave is very small due to coverage of the GC surface and shifts to the negative potential region. The wave completely disappears on the third scan. This is attributed to the electrografting of 3,8-BCC and 3,8-BCCNO molecules onto the GC surface and the blocking of further reduction of the diazonium salt species in solution. In a previous paper, the surface modification of GC [11, 43], platinum [14] and gold [15] electrodes with 2-BCC DAS was investigated and very similar electrochemical behavior was observed.

It is interesting to compare the modification voltammograms of the 3,8-BCC and 3,8-BCCNO bisdiazonium salts. E_p and I_p values for the first scans are substantially different for -N=N- and –N=NO- derivatives. The reduction peak potential for 3,8-BCCNO-BDAS (−0.336 V) is almost 120 mV more negative than for 3,8-BCC-BDAS (-0.216 V). This difference between reduction potentials is attributed to the electron-donating ability via the mesomeric effect of the oxygen atom in the N-oxide derivative. In the case of –N=NO- derivative, the diazo groups become less positively charged compared to the -N=N- derivative, and the reduction potential shifts to more negative values. The peak current for the 3,8-BCCNO-BDAS reduction is also lower than that for the 3,8-BCC-BDAS, reflecting the limitation of the electron transfer to the less positively charged diazo group. The efficiency of grafting radicals to the GC surface is high in both cases, as can be understood by the passivation of the surface during subsequent scans of modification (Fig. 1).

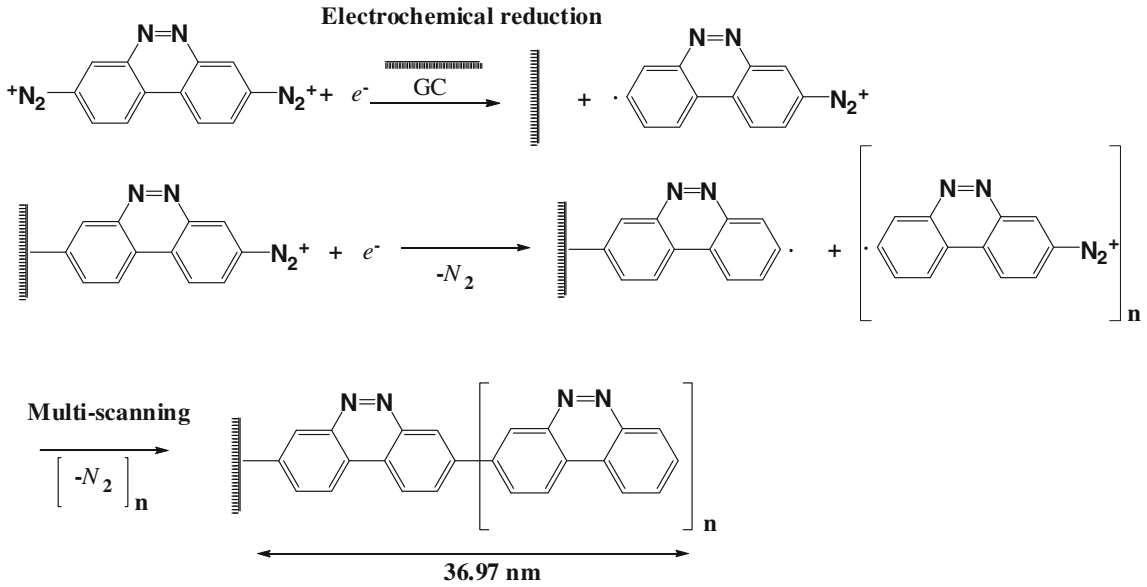

Scheme 1 Modification mechanism of 3,8-BCC bisdiazonium salt at the glassy carbon surface (in MeCN containing 0.1 M TBATFB)

Electrochemical evidence for 3BCC-GC and 3BCCNO-GC surfaces using cyclic voltammetry. Cyclic voltammetry (CV) is a very important technique for evaluating the blocking property of the organic-coated electrodes using diffusion controlled redox couples as probes [44]. GC electrodes were modified with 1 mM 3,8-BCC-BDAS and 3,8-BCCNO-BDAS in MeCN with 0.1 M TBATFB as background electrolyte via the electrochemical reduction process as mentioned above. Passivation of the GC surfaces after modification was confirmed using four kinds of redox molecules with different electrochemical behaviors in various media. The redox molecules used were potassium ferricyanide (2 mM in 0.1 M KCl), hexammineruthenium(III) chloride (HRu) (2 mM in 0.1 M KCl), ferrocene (Fc) (2 mM in 0.1 M TBATFB in MeCN) and dopamine (DA) (2 mM in 0.1 M H_2SO_4). These redox probes were used to characterize the 3BCC and 3BCCNO films thought to be on the glassy carbon surface after the modification process.

Ferricyanide and ferrocene are blocked on the 3BCC and 3BCCNO modified GC surfaces. The response of the surface against DA and HRu chloride is similar to the behavior of ferrocene and ferricyanide redox probes, blocking the electron transfer at the 3BCC-GC and 3BCCNO-GC surface. CV voltammograms showed that GC surfaces were covered with 3-BCC and 3-BCCNO molecules and that the electrochemical reactions of all redox probes were completely blocked in both aqueous and nonaqueous media. Blockage of the redox probes (dopamine, hexammineruthenium chloride, ferricyanide and ferrocene) shows that the film on the 3BCC and 3BCCNO modified GC surface is compact, dense and without pinholes nor defects [13, 14, 45].

Attachment of 3BCC to the GC surface can be investigated using the complexation ability of the surface by Cu^{2+} ions. Cu^{2+} ions were deposited on the 3BCC-GC electrode by immersing the electrode into a solution

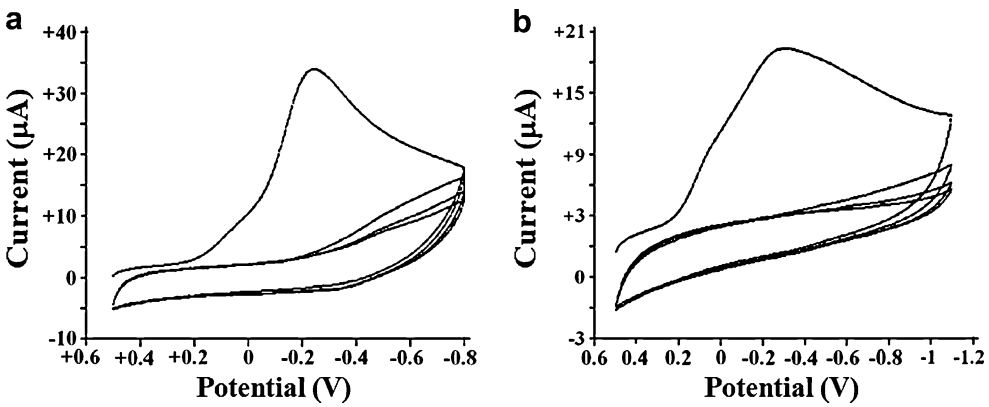

Fig. 1 **a** Cyclic voltammograms of 1 mM 3,8-benzo[*c*]cinnoline and **b** 1 mM 3,8-benzo[*c*]cinnoline 5-oxide bisdiazonium salts at the GC surface in acetonitrile containing 0.1 M TBATFB vs. Ag/Ag^+ (0.01 M). Scan rate is 200 mV s^{-1}

containing Cu^{2+} ions. Deposition of the Cu^{2+} ions was carried out by the complexation in a 2×10^{-3} M $CuCl_2$ solution (0.1 M KCl) overnight, producing the Cu/3BCC-GC electrode. This formed electrode was taken out of the Cu^{2+} solution and rinsed with pure water to remove any extraneous adsorbed species. Cyclic voltammograms of the copper complexed surface were acquired in a 0.1 M KCl solution.

Figure 2 shows the cyclic voltammograms of the surface confined complex and the Cu^{2+}/BCC complex in an acetonitrile (0.1 M TBATFB) solution. Reversible voltammograms are assigned for the $Cu^{2+/1+}$ redox couple in the complex.

Peak separation for the complex in solution is approximately 300 mV. On the other hand, peak separation for the surface confined complex is about 10 mV, implying the electroactive adsorbed species [1]. This behavior is clear evidence of the complexation of Cu^{2+} ions with the 3BCC species at the GC surface.

Development and validation of the quantitative method for the determination of metal ions is under investigation and is the subject of another paper. These types of modified electrodes can be used as chemical sensors for organic and inorganic substances.

Characterization of 3BCC-GC and 3BCCNO-GC surfaces using XPS spectroscopy

To evaluate the composition of the 3BCC-GC and 3BCCNO-GC surfaces, XPS analysis was performed. The XPS survey spectra of the surfaces are shown in Fig. 3. Signals for carbon, nitrogen and oxygen atoms were

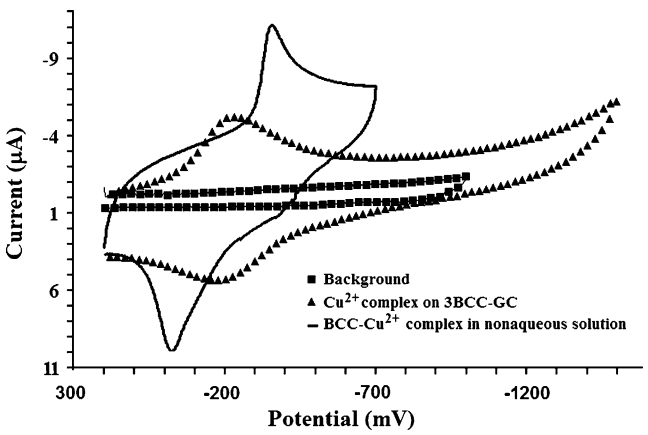

Fig. 2 Cyclic voltammograms of acetonitrile (0.1 M TBATFB) background on 3BCC-GC (■); Cu^{2+}/BCC complex in acetonitrile (0.1 M TBATFB) solution on GC (—); Cu^{2+} adsorbed on 3BCC-GC in acetonitrile (0.1 M TBATFB) solution (▲). Scan rate is 100 mV s^{-1}

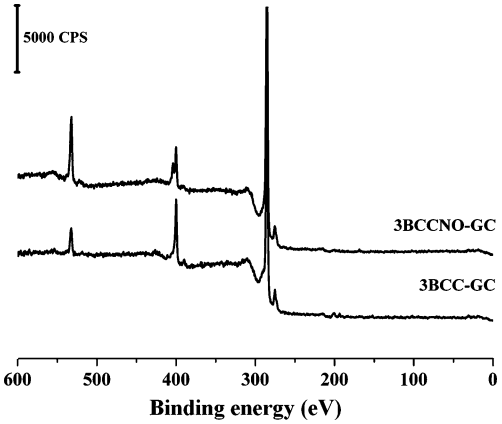

Fig. 3 XPS survey spectra of 3BCC-GC and 3BCCNO-GC surfaces

detected in the survey spectra. Careful examination of the survey spectra reveals that the main differences in the XPS spectra of both surfaces are the shape of N_{1s} peaks and the intensity of O_{1s} peaks.

Narrow region N_{1s} spectra for 3BCC-GC and 3BCCNO-GC surfaces are given in Fig. 4. The XPS peak at 400.0 eV that is present for the two compounds could be attributed to azo groups present in the organic layer as also shown for monodiazonium salts [46, 47]. The presence of such azo groups has also been confirmed by ToF-SIMS and IR [48]. The N_{1s} peak of the 3BCC-GC surface is observed at 399.9 eV and attributed to the -N=N- nitrogen of 3BCC film at the GC surface. Inspection of the N_{1s} spectra of the 3BCCNO-GC surface reveals two N_{1s} peaks are detected at 404.0 eV and 400.0 eV [11]. The peak at 400.0 eV is attributed to the -N=NO- and nitrogen which is shifted to a higher binding energy value with the inductive effect of oxygen attached to the nearby nitrogen. The peak at 404.0 eV is attributed to the oxygen bearing nitrogen of 3BCCNO film, -N=NO-.

This feature is very informative, showing grafting of 3BCC and 3BCCNO films at the GC surfaces.

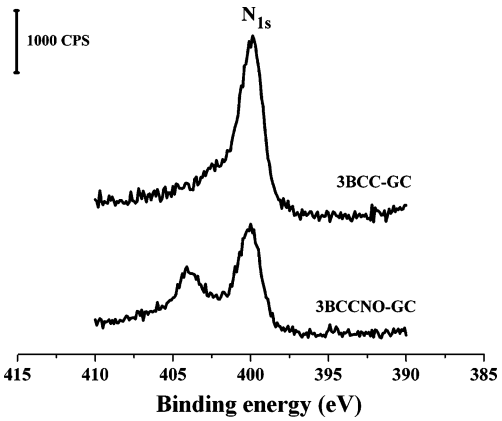

Fig. 4 Narrow region N_{1s} spectra of 3BCC-GC ve 3BCCNO-GC surfaces

The O_{1s} feature is detected at 532.3 eV and 532.1 eV for 3BCC-GC and 3BCCNO-GC surfaces, respectively. The presence of a small O_{1s} peak for 3BCC-GC is attributed to oxygen at the GC surface due to atmospheric oxidation and/or structural contamination during fabrication [49, 50]. Immobilization of 3,8-benzo[*c*]cinnoline N-oxide on a GC surface results in intensity changes as well as binding energy shifts in the O_{1s} peak. The high-resolution O_{1s} spectrum of the peak can be deconvoluted into two main peaks: the oxygen atoms attached to the N atom in the structure of the molecule (533.1 eV), -N=NO- and the oxygen species present due to atmospheric oxidation of GC (531.9 eV) (Fig. 5). The presence of the oxygen peaks clearly verifies the binding of 3BCCNO to the GC surface. Furthermore, the increased oxygen concentration at the 3BCCNO-GC surface might be attributed to the oxygen of the -N=NO- group in addition to surface contaminated oxygen.

Characterization of 3BCC-GC and 3BCCNO-GC surfaces using IRRAS

In addition to electrochemical and XPS analyses, IRRAS spectroscopy was used to get information about the structure of the modified surfaces from their vibrational transitions. IR signals for pure solids 3,8-BCC and 3,8-BCCNO bisdiazonium salts and 3,8-benzo[*c*]cinnoline and 3,8-benzo[*c*]cinnoline 5-oxide modified GC surfaces were taken in the frequency range of 600 cm^{-1}–4000 cm^{-1}, given in Fig. 6. The spectrum of the bare GC surface was subtracted from the spectrum of the modified surfaces to obtain the IR spectrum of 3BCC and 3BCCNO films. IR bands for the 3BCC film at the GC surface and solid 3,8-BCC-BDAS were observed at 750 cm^{-1} and 768 cm^{-1} (C-H out of plane bending), 1347 cm^{-1} for both spectra (C-N stretch), 1457 cm^{-1} and 1456 cm^{-1} (C-N=N + ring deformation), respectively. The IR spectra of 3BCCNO film and solid 3,8-BCCNO-BDAS show also bands at 767 cm^{-1} and 820 cm^{-1} (C-H out of plane bending), 1371 cm^{-1} and 1333 cm^{-1} (C-N stretch), 1464 cm^{-1} and 1459 cm^{-1} (C-N=N + ring deformation). The aromatic ring stretching vibrations were observed at 1596 cm^{-1} and 1576 cm^{-1} for 3BCC-GC and 3BCCNO-GC surfaces and these bands were also seen in the spectra of 3,8-BCC-BDAS and 3,8-BCCNO-BDAS at 1599 cm^{-1} and 1601 cm^{-1}, respectively. The N-oxide group band was observed at 1241 cm^{-1} for 3BCCNO-GC surface and 1260 cm^{-1} for 3,8-BCCNO-BDAS [51]. The IR signals of the -N≡N- stretching bands for 3,8-BCC-BDAS and 3,8-BCCNO-BDAS observed at 2306 cm^{-1} were not observed at the spectrum of 3BCC and 3BCCNO films as expected [52–54]. The broad and intense band around 1070 cm^{-1}, which indicates the anionic BF_4^- group of the diazonium salts, clearly not observed in the spectrum of 3BCC-GC and 3BCCNO-GC surfaces. The region between 1500 and 2500 cm^{-1} shows the largest spectral difference between the solid 3,8-BCC-BDAS and 3,8-BCCNO-DAS in KBr disk and surface confined 3BCC and 3BCCNO films, which was interpreted as the disapperance of -N≡N- groups due to electrochemical reduction of one and elimination of the other by hydro-dediazoniation [42]. The C-N stretches were observed at 1347 cm^{-1} and 1347 cm^{-1} for 3BCC film and 3,8-BCC-BDAS salt; at 1371 cm^{-1} and 1333 cm^{-1} for 3BCCNO film and 3,8-BCCNO-BDAS salt.

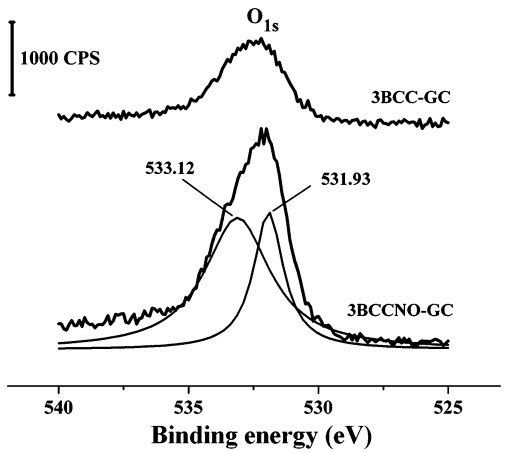

Fig. 5 Narrow region O_{1s} spectra of 3BCC-GC ve 3BCCNO-GC surfaces

Characterization of 3BCC-GC and 3BCCNO-GC surfaces using EIS

Electrochemical impedance spectroscopy (EIS) is a suitable technique for monitoring of surface properties. It is capable of giving useful information about defects/holes of the modified surface, the kinetics and mechanism of the film formation processes, surface coverage, and so forth [55–57]. Methodology used with this technique is always based on a comparison of the results that obtained with the unmodified and modified electrode surfaces.

This study used EIS to examine surface integrity, pinhole density and the distribution of regions occupied by BCC and BCCNO molecules using surface layer kinetics for an $Fe(CN)_6^{3-/4-}$ redox probe in 0.1 M KCl in an aqueous medium. An $Fe(CN)_6^{3-/4-}$ couple is an outer sphere redox system and can therefore be used as a redox probe in EIS to analyze pinholes and defects on modified surfaces [14, 58]. Figure 7 shows the impedance plots (Nyquist plots) of the bare GC, the 3BCC-GC and the 3BCCNO-GC modified electrodes. Bare GC shows almost a straight line impedance plot. On the other hand, the 3BCC and 3BCCNO modified GC electrodes show a semicircle at the high frequency region, implying

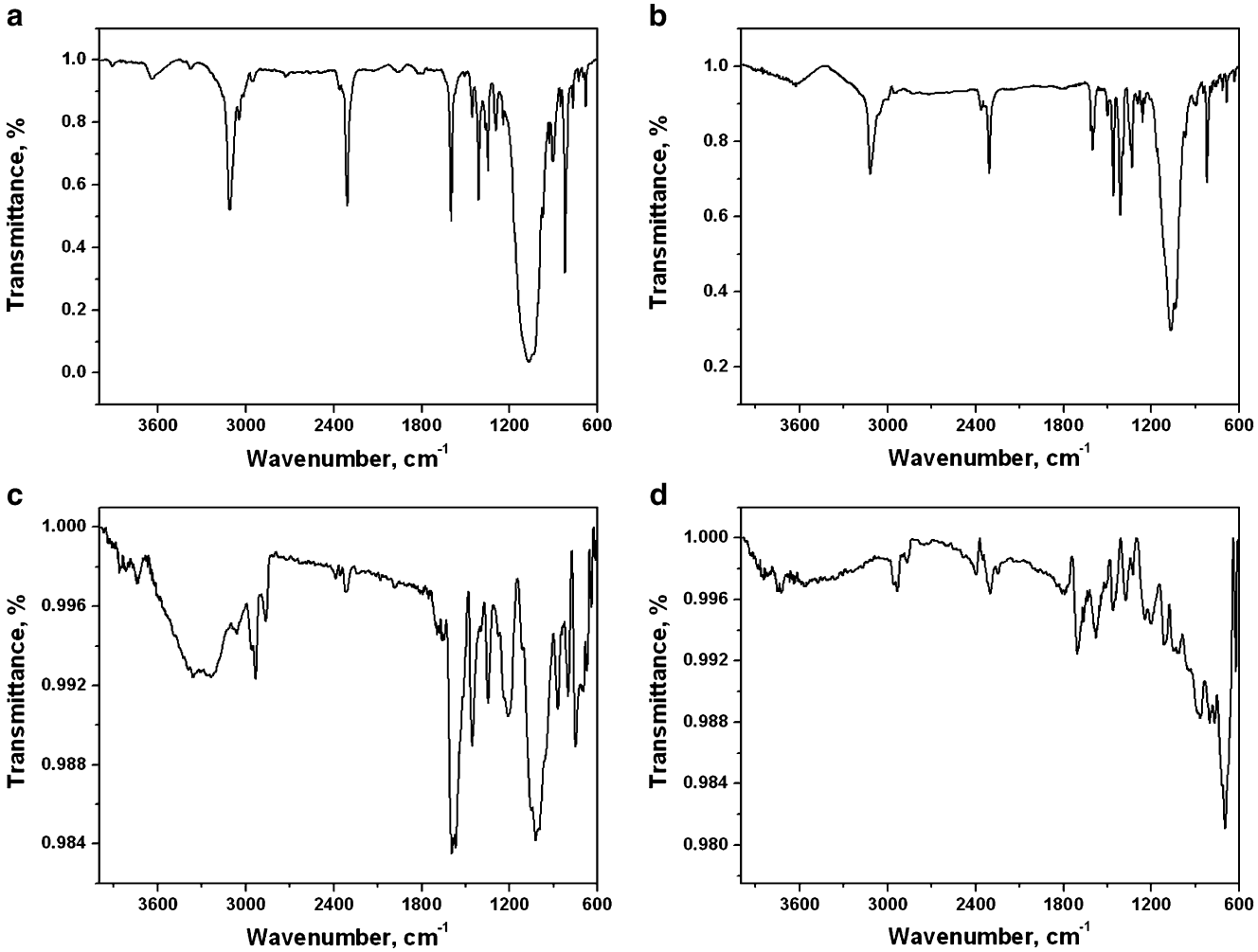

Fig. 6 FTIR (*absorption*) spectrum of (**a**) 3,8-BCC-BDAS, (**b**) 3,8-BCCNO-BDAS, (**c**) IRRAS (*reflectance*) spectrum of 3BCC-GC and (**d**) 3BCCNO-GC surfaces

that these surfaces can block ability for the $Fe(CN)_6^{3-/4-}$ electron transfer kinetics.

Figure 7 (a,b) shows the experimental data obtained that are fitted to standard Randles equivalent circuits for 3BCC-GC and 3BCCNO-GC analysis, which comprises the solution resistance (R_s), the charge-transfer resistance (R_s), the Warburg resistance (Z_w), and the constant phase element (CPE) for the cases of bare GC and 3BCC-GC and 3BCCNO-GC electrodes. The experimental impedance values are matched with Randles equivalent circuit simulations using Gamry EIS300 software as described in our previous paper [14]. Best fit Nyquist plots in Fig. 7 show a semicircle transformed into a rising curve, but with a slope less than unity, suggesting ineffective diffusion of $Fe(CN)_6^{3-/4-}$ ions to the film due to poor porosity. At the low frequency region, the curve shows a competition between diffusion and charge transfer reaction. R_{ct}° and R_{ct} values were calculated from the impedance plots for $Fe(CN)_6^{3-/4-}$ at the bare GC, 3BCC-GC and 3BCCNO-GC electrodes as 131.6 Ω cm^2, 42.54 kΩ cm^2 and 25.95 kΩ cm^2, respectively. Charge transfer resistances at the 3BCC-GC and 3BCCNO-GC surfaces were higher than at the bare GC electrode, indicating the presence and blocking property of films at the GC surface. The 3BCC film appears more compact, dense and thicker than the 3BCCNO film.

To calculate the appearant electron transfer rate constant k_{app} at the bare GC and the modified electrodes, the equation

$$R_{ct} = \frac{RT}{(nF)^2 A k_{app} C} \tag{1}$$

can be employed in the high frequency part of the spectra, where A is the electrode area, n is the number of electrons transferred, C is the concentration of the redox probe system and all other symbols have their usual meanings [14, 59, 60]. Apparent rate constant values of 8.1×10^{-8} cm s^{-1} and 1.3×10^{-7} cm s^{-1} were determined at the 3BCC-GC and 3BCCNO-GC electrodes, respectively.

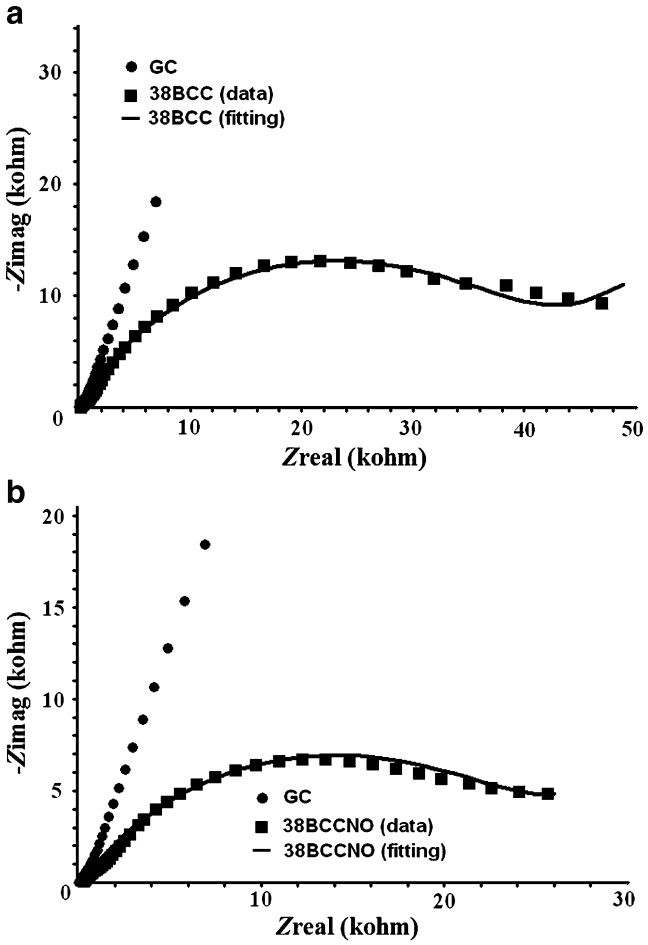

Fig. 7 Fitting of impedance plot for the $Fe(CN)_6^{3-/4-}$ system in 0.1 M KCl on the **(a)** 3BCC-GC and **(b)** 3BCCNO-GC surfaces. Dotted curve is the experimental Nyquist plot while the solid one is Nyquist plot for the Randles equivalent circuit. Frequency range is 100 kHz to 0.1 Hz

Charge transfer resistance values also permit evaluation of the surface coverages (θ) of the surfaces using Eq. 2 [14, 61, 62].

$$\theta = 1 - \frac{R_{ct}^{\circ}}{R_{ct}} \tag{2}$$

The surface coverage values determined from the above equation are 99.977% for 3BCC-GC and 99.962% for 3BCCNO-GC, which are expected values for compact and dense films.

Ellipsometric measurements of film thicknesses

Table 1 shows the 3BCC and 3BCCNO film thicknesses at the GC surface measured by ellipsometry. Measurements were performed at five different locations to check the homogeneity of the modified surfaces. Mean values of film thickness are 36.97±0.92 nm and 19.27±0.68 nm for 3BCC and 3BCCNO films, respectively. Distribution of the thicknesses at five locations indicates a significant homogeneity of the nanofilms. Fitting was based on a four-phase model consisting of Graphite/Glassy Carbon/organic film/air. Refractive indices were 3.0841 for graphite, 1.900 for GC, 1.460 for the 3BCC and 3BCCNO layers and 1.000 for air, assuming that thickness and refractive indices are reasonably corrolated for all films. Extinction coefficients (k) are −1.782 for graphite, −0.810 for GC and 0.000 for organic films and air. It will be interesting to compare the film thicknesses for 3BCC and 3BCCNO.

Table 1 Ellipsometric thickness of the 3BCC film on GC surface

Spot 1	Spot 2	Spot 3	Spot 4	Spot 5
3BCC film thicknesses[a]				
38.42	36.13	37.10	36.15	36.40
36.14	36.07	38.02	38.46	36.22
37.06	36.03	37.20	36.02	36.01
38.34	38.34	37.20	36.07	37.17
36.05	37.10	37.21	38.38	37.14
3BCCNO film thicknesses[b]				
18.22	19.44	19.44	18.10	20.00
20.03	18.17	19.20	20.03	19.25
19.20	19.33	18.42	18.17	20.13
19.33	19.25	20.08	20.03	19.98
18.42	19.22	19.22	19.17	20.00

[a] Mean thickness=36.97 nm
Std. dev=0.92 nm
[b] Mean thickness=19.27 nm
Std. dev=0.68 nm

In the formation of multilayer process, as outlined in Scheme 1, it is probable that one of the diazo group of 3,8-BCC-BDAS is exhaustively reduced by one electron reduction, forming an aryl radical. The aryl radical attacks the GC surface, probably forming a monolayer, which blocks the further reduction of the molecules in solution. This phenomenon is easily understood from the 1st cycle modification CV, as shown in Fig. 1. During the 1st scan, the diazo groups of the molecules grafted to the surface are also reduced at the same potential with the species in solution, forming surface confined radicalic species. The surface confined radicalic species are attacked by the BCC radicals formed in solution, producing a bilayer film. In this fashion, deposition of BCC molecules continues until a specified thickness is reached, resulting in a multilayer film with the terminal diazo groups. The terminal diazo groups of the 3BCC film undergo the hydro-dediazoniation process wherein the diazo groups are replaced by a proton from the proton donor, probably the residual water present in acetonitrile [61, 62]. Ellipsometric measurements clearly show the multilayer character of the 3BCC and 3BCCNO films with thicknesses of 36.97 nm and 19.27 nm,

respectively. Another evidence of the film thickness difference comes from EIS data of charge transfer resistance (R_{ct}) values for 3BCC and 3BCCNO films. R_{ct} is higher for the 3BCC film than for the 3BCCNO film, which means that the thickness of the former film is higher than that of the later.

Stability and working range of modified electrodes

The stability of the 3BCC and 3BCCNO nanofilms was tested by CV voltammograms using dopamine as a redox probe. Stability was examined for open atmosphere influence, water solubility and potential scan range. CV voltammogram of dopamine was acquired after the electrodes was subjected to cathodic and anodic potential limits to observe desorption of the film, and hence the formation of pinholes. Gradual potential excursions to the negative direction in a 0.1 M H_2SO_4 had a marked influence of desorption of the surface films after −1.0 V for both surfaces, as shown by the appearence of a DA oxidation current. The same experiment was performed to find out the positive potential limit of both surfaces by gradually scanning in a positive direction. 3BCC-GC and 3BCCNO-GC surfaces were found to be stable up to +1.8 V excursions in the positive side and −1.0 V excursions in the negative side. Therefore, both electrodes can be safely used in electroanalytical measurements in a potential range of from +1.8 V to −1.0 V. The stability of a variety of surfaces prepared by diazonium salt reduction against relatively high negative and positive potentials has been reported in the literature, which is in accordance with our results [12, 14, 15, 63]. When the modified surface was kept in pure water the surfaces were stripped out within 3 days while in open atmosphere surface stripping took more than 20 days.

Conclusions

3,8-BCC-BDAS and 3,8-BCCNO-DAS were synthesized and successfully electrografted onto GC surfaces. The presence of modifiers at the GC surface was confirmed using CV, EIS, XPS, IRRAS and ellipsometry. The stability of the modified 3BCC-GC and 3BCCNO-GC surfaces was checked by scanning the potential to very cathodic and very anodic limits using dopamine voltammetry. It was found that 3BCC-GC and 3BCCNO-GC electrodes can safely be used in electroanalytical measurements in a potential range of from +1.8 V to −1.0 V. The thicknesses and homogeneities of the multilayer films were investigated using ellipsometric measurements. Ellipsometric thicknesses of 3BCC and 3BCCNO films were determined as 36.97 nm and 19.27 nm with standard deviations of 0.92 nm and 0.68 nm at three different locations, respectively. Analytical application of these novel surfaces for copper ion determination was also investigated. A multilayer formation mechanism was proposed based on electrochemical, ellipsometric and spectroscopic data.

Acknowledgments This work was supported by the Ankara University Scientific Research Fund with Project Grant numbers of 2000-07-05-019 and 2003-07-05-084 and by the TUBITAK (Scientific and Technological Research Council of Turkey) project with a number of 106T622.

References

1. Bard AJ (1994) Integrated chemical systems: a chemical approach to nanotechnology. John Wiley&Sons, New York
2. Delamar M, Désarmott G, Fagebaumme O, Hitmi R, Pinson J, Savéant J-M (1997) Carbon 35(6):801–807
3. Nöll G, Kozma E, Grandorj R, Carey J, Schödl T, Hauska G, Daub J (2006) Langmuir 22:2378–2383
4. Downard AJ, Prince MJ (2001) Langmuir 17:5581–5586
5. Adenier A, Bernard MC, Chehimi MM, Cabet-Deliry E, Desbat B, Fagebaume O, Pinson J, Podvorica F (2001) J Am Chem Soc 123:4541–4549
6. Downard AJ (2000) Electroanalysis 12(14):1085–1096
7. Dalmolin C, Canobre SC, Biaggio SR, Rocha-Filho RC, Bocchi N (2005) J Electroanal Chem 578(1):9–15
8. Dong H, Zheng H, Lin L, Ye B (2006) Sens Actuators B 115 (1):303–308
9. Pinson J, Podvorica F (2005) Chem Soc Rev 34:429–439
10. Solak AO, Eichorst LR, Clark WJ, McCreery RL (2003) Anal Chem 75:296–305
11. İsbir AA, Solak AO, Üstündağ Z, Bilge S, Natsagdorj A, Kılıç E, Kılıç Z (2005) Anal Chim Acta 547(1):59–63
12. İsbir AA, Solak AO, Üstündağ Z, Bilge S, Kılıç Z (2006) Anal Chim Acta 573–574:26–33
13. İsbir-Turan AA, Üstündağ Z, Solak AO, Kılıç E, Avseven A (2008) Electroanalysis 20(15):1665–1670
14. İsbir-Turan AA, Üstündağ Z, Solak AO, Kılıç E, Avseven A (2009) Thin Solid Films 517(9):2871–2877
15. Üstündağ Z, İsbir-Turan AA, Solak AO, Kılıç E, Avseven A (2009) Instrum Sci Technol 37(3):284–302
16. Combellas C, Kanoufi F, Pinson J, Podvorica FI (2005) Langmuir 21:280–286
17. McCreery RL, Viswanathan U, Prasad Kalakodimi R, Nowak AM (2006) Faraday Discuss 131:33–43
18. Palacin S, Bureau C, Charlier J, Deniau G, Mouanda B, Viel P (2004) Chemphyschem 5:1468–1481
19. Harper JC, Polsky R, Wheeler DR, Brozik SM (2008) Langmuir 24:2206–2211
20. Gooding JJ (2008) Electroanalysis 20(6):573–582
21. Ping H, Zhiqiang X, Juntao L (1996) J Electroanal Chem 405 (1–2):217–221
22. Ranganathan S, McCreery RL (2001) Anal Chem 73:893–900
23. Morita K, Yamaguchi A, Teramae N (2004) J Electroanal Chem 563(2):249–255
24. Zhou J, Wipf DO (1997) J Electrochem Soc 144(4):1202–1207
25. Sullivan MG, Schnyder B, Bärtsch M, Alliata D, Barbero C, Imhof R, Kötz R (2000) J Electrochem Soc 147(7):2636–2643
26. Fukuda N, Mitsuishi M, Aoki A, Miyashita T (2002) J Phys Chem B 106(28):7048–7052
27. Kalk W, Schuendehuette KH (1972) DE2041689

28. Wolf GD, Miessen R, Nischk G (1975) DE2404460
29. Etienne A, Le Berre A, Brun JJ (1969) FR1576505
30. Gerald J (1980) DE2939259
31. Hirose H, Watanabe K, Kinoshita A (1986) JP61259257
32. Oomura S, Go S, Tanaka M (1992) JP4256960
33. Leary JA, Lafleur AL, Liber HL, Biemann K (1983) Anal Chem 55(4):758–761
34. Entwistle ID, Gilkerson T, Barton JW (1981) GB2059263
35. Etienne A, İzoret G (1964) Bull Soc Chim Fr 11:2897–2901
36. Kılıc E, Tüzün C (1990) Org Prep Proced Int 22(4):485–493
37. Paradisi C, Gonzalez-Trueba G, Scorrano G (1993) Tetrahedron Lett 34(5):877–878
38. Bjorsvik HR, Gonzalez RR, Liguori L (2004) J Org Chem 69 (22):7720–7727
39. Ullmann F, Dieterle P (1904) Berichte 22:23–36
40. Braithwaite RSW, Holt PF, Hughes AN (1958) J Chem Soc 4073–4077
41. Anariba F, Viswanathan U, Bocian DF, McCreery RL (2006) Anal Chem 78:3104–3112
42. Clark AJ, Rooke SM (2003) In: Knipe AC, Watts WE (eds) Organic reaction mechanisms in radical reactions. John Wiley&Sons, New York
43. Üstündağ Z, Solak AO (2009) Electrochim Acta 54(26):6426–6433
44. Cruickshank AC, Tan ESQ, Brooksby PA, Downard AJ (2007) Electrochem Commun 9:1456–1462
45. Matrab T, Hauquier F, Combellas C, Kanoufi F (2010) Chemphyschem 11:670–682
46. Saby C, Ortiz B, Champagne GY, Bélanger D (1997) Langmuir 13:3837–3844
47. Hurley BL, McCreery RL (2004) J Electrochem Soc 151:B252–B259
48. Doppelt P, Hallais G, Pinson J, Podvorica F, Verneyre S (2007) Chem Mat 19:4570–4575
49. McCreery RL (2008) Chem Rev 108(7):2646–2687
50. Jaramillo A, Spurlock LD, Young V, Brajter-Toth A (1999) Analyst 124:1215–1221
51. Hwu JR, Das AR, Yang CW, Huang J-J, Hsu M-H (2005) Org Lett 7(15):3211–3214
52. Yasseri A, Syomin D, Malinovskii V, Loewe R, Lindsey J, Zaera F, Bocian DF (2004) J Am Chem Soc 126:11944–11953
53. Wei L, Syomin D, Loewe R, Lindsey JS, Zaera F, Bocian DF (2005) J Phys Chem B 109:6323–6330
54. Yasseri A, Syomin D, Loewe R, Lindsey J, Zaera F, Bocian DF (2004) J Am Chem Soc 126:15603–15612
55. Macdonald DD (2006) Electrochim Acta 51(8–9):1376–1388
56. Pedrosa VA, Suffredini HB, Codognoto L, Tanimoto ST, Machado SAS, Avaca LA (2005) Anal Lett 38(7):1115–1125
57. Jin G, Lin X, Gong J (2004) J Electroanal Chem 569(1):135–142
58. Chen P, McCreery RL (1996) Anal Chem 68(22):3958–3965
59. Oliveira-Brett AM, da Silva LA, Brett CMA (2002) Langmuir 18 (6):2326–2330
60. Ganesh V, Pal SK, Kumar S, Lakshminarayanan V (2006) J Colloid Interf Sci 296:195–203
61. Doubova LM, Daolio S, Pagura C, de Battisti A, Trasatti S (2003) Russ J Electrochem 39(2):164–169
62. Sawyer DT, Sobkowlak A, Roberts JL (1995) J Electrochemistry for Chemists Ch. 7, Wiley-Interscience Pub, New York
63. Amours MD, Bélanger D (2003) J Phys Chem B 107(20):4811–4817